Measurements of the Antineutrino Spin Asymmetry in Beta Decay of the Neutron and Restrictions on the Mass of a Right-Handed Gauge Boson

I. A. Kuznetsov, A. P. Serebrov, I. V. Stepanenko, A. V. Alduschenkov, M. S. Lasakov, and A. A. Kokin
Petersburg Nuclear Physics Institute, 188350, Gatchina, Russia

Yu. A. Mostovoi
Kurchatov Institute, 123182, Moscow, Russia

B. G. Yerozolimsky
Department of Physics, Harvard University, Cambridge, Massachusetts, 02138

M. S. Dewey
National Institute of Standards and Technology, Gaithersburg, Maryland 20899
(Received 20 December 1994)

We report a new measurement of the neutron antineutrino spin asymmetry coefficient B in the beta decay of polarized neutrons. Combining results of measurements of the observed asymmetry $PB = 0.6617 \pm 0.0044$ with measurements of the neutron beam polarization $P = (66.88 \pm 0.22)\%$, we obtain the value $B = 0.9894 \pm 0.0083$. This value implies that the mass of a hypothetical right-handed charged gauge boson in the left-right symmetric model of the weak interaction is greater than 281 GeV/c^2 (90% C. L.). This is in agreement with restrictions from muon decay and direct searches for an additional vector boson W'.

PACS numbers: 14.70.Pw, 13.30.Ce, 23.40.Bw

Precise measurements of neutron beta decay parameters can be used to test the standard model of weak interactions. Recently, the accuracy of measurements of the neutron lifetime (τ) and electron spin asymmetry (A) have been improved considerably thereby improving the accuracy with which the vector and axial vector coupling constants of weak interactions (g_v and g_a) can be derived. However, the vector coupling constant g_v obtained from neutron data is in poor agreement with g_v obtained from superallowed nuclear $0^+ \rightarrow 0^+$ transitions [1–3]. Analysis of this discrepancy together with data from ^{19}Ne in the framework of the left-right model of weak interactions is consistent with a finite mass for W_R of 230 GeV/c^2 [2,3]. This is in contradiction with restrictions from muon decay and direct searches for additional vector boson W' [4,5] under the assumption that associated right-handed neutrinos are not massive. A measurement of the antineutrino spin asymmetry in neutron beta decay with an accuracy of less than 1% would be sufficient to strongly confirm or refute this restriction [3].

The work described here was carried out on the vertical channel of cold polarized neutrons at the WWR-M reactor at the Petersburg Nuclear Physics Institute, Gatchina, Russia where the neutron flux is 2×10^8 neutrons cm^2/s.

The scheme for this measurement was first proposed in Ref. [6]. Measurements of momentum and angle of escape of the undetected antineutrino are possible due to coincident detection of the electron and recoil proton and subsequent measurement of their momenta. A kinematic diagram of beta decay is shown in Fig. 1. For a given electron energy, the antineutrino energy can be deduced with an accuracy of better than 0.75 keV, the maximum proton recoil energy. For a given electron momentum, all possible values of antineutrino momentum lie on a sphere of radius $P_\nu = (E_0 - E_e)/c$, where P_ν is the antineutrino momentum, E_0 is the total kinematic energy of decay, and E_e is the electron energy. By further measuring the x projection of proton momentum P_{px} (see Fig. 1) using time of flight, we can determine the antineutrino escape angle and reconstruct the beta decay event. The finite sizes of the

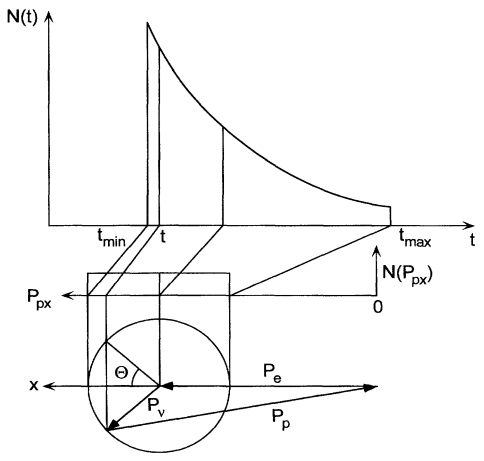

FIG. 1. The momentum diagram of neutron decay products and time of flight spectrum of protons for ideal conditions. P_e, P_ν, and P_p are momenta of the electron, antineutrino, and recoil proton. P_{px} is the x component of P_p.

 0031-9007/95/75(5)/794(4)$06.00

decay region and electron detector and imperfect response functions for the electron and proton complicate matters and force us to use a Monte Carlo procedure to realize the mean value of the antineutrino escape angle.

The events detected in this experiment can be assigned to a matrix of coincidence with coordinates E_e and t_p for the two opposite directions of beam polarization (+ and −). The event rate for each cell of this matrix is given by

$$N_{ik}^{\pm} = f(E_i)\Big[1 + a\frac{v_i}{c}\langle\cos\Theta_{e\nu}\rangle_{ik} \pm PA\frac{v_i}{c}\langle\cos\Theta_{\sigma e}\rangle_{ik} \pm PB\langle\cos\Theta_{\sigma\nu}\rangle_{ik}\Big], \quad (1)$$

taking into account the correlation coefficients of beta decay. This yields the experimental asymmetry

$$X_{ik} \equiv \frac{N_{ik}^{+} - N_{ik}^{-}}{N_{ik}^{+} + N_{ik}^{-}} = \frac{PA(v_i/c)\langle\cos\Theta_{\sigma e}\rangle_{ik} + PB\langle\cos\Theta_{e\nu}\rangle_{ik}}{1 + a(v_i/c)\langle\cos\Theta_{e\nu}\rangle_{ik}}, \quad (2)$$

and finally

$$PB = \frac{\{X_{ik}[1 + a(v_i/c)\langle\cos\Theta_{e\nu}\rangle_{ik}]\} - AP(v_i/c)\langle\cos\Theta_{\sigma e}\rangle_{ik}}{\langle\cos\Theta_{\sigma\nu}\rangle_{ik}}. \quad (3)$$

In these equations a, A, and B are coefficients of electron antineutrino asymmetry, electron spin asymmetry, and antineutrino spin asymmetry [7], P is the degree of neutron polarization, v_i is the electron velocity, and $f(E_i)$ combines the phase-space factor and Fermi function. The subscripts i and k denote a definite interval of electron energy E_i and time of flight of the proton t_k. To determine B it is necessary to know the beam polarization and calculated values for $(v/c)\langle\cos\Theta_{e\nu}\rangle$, $(v/c)\langle\cos\Theta_{\sigma e}\rangle$, and $\langle\cos\Theta_{\sigma\nu}\rangle$. The values of the correlation coefficients a and A are known from previous experiments [8,9]. The terms with coefficients a and A are small ($\lesssim 0.1$), so the experimental uncertainties on a and A do not contribute significantly to the total error of PB.

To calculate the mean cosine values, a Monte Carlo model of the beta decay process inside the apparatus is used. The model includes all the necessary geometrical parameters of the chamber, the responses of the electron and proton detectors, the measured distribution of neutron intensity inside the beam, the shape of the electron spectrum in the form of the Fermi function, and the characteristics of the amplitude to digital (ADC) and time to digital (TDC) converters. A relaxation calculation is used to obtain the electric field inside the apparatus.

A diagram of the apparatus is shown in Fig. 2. The decay region (4) is defined by means of a diaphragm in front of the electron detector. Coincident signals from the electron (1) and proton (2) detectors, which are located on opposite sides of the decay region, are registered for each direction of neutron polarization. The electron detector is a photomultiplier with a plastic scintillator. The energy resolution and fraction of backscattering of electrons for this detector were determined in a separate experiment by means of a magnetic beta spectrometer [9].

Decay protons passing through the time of flight cylinder (6) at first maintain their velocities. Then they are accelerated and focused onto the proton detector by an electric field with potential 25.6 kV applied between the spherical electrode (7) and spherical grid (8). The proton detector is an assembly of two microchannel plates. In this configuration, it is possible to determine the time of arrival of each proton to an accuracy of 10 ns.

The entire chamber is surrounded by three pairs of current carrying frames to null the Earth's magnetic field and to provide a 0.05 mT guiding magnetic field in the chamber. The residual Earth's field is less than 1 μT. The polarization reversal is accomplished with a radio frequency flipper. To avoid any possible influence of the flipper on the photomultiplier, the guiding magnetic field and the magnetic field of the flipper are reversed once every 12 h.

Pulses from the electron detector are used to start a TDC and to provide the electron energy. Pulses from the proton detector stop the TDC thereby providing a time of flight measurement. The method of delayed coincidence is used to determine the background. The background is measured simultaneously with the coincidence signal using the same electronic processing. During 93 h

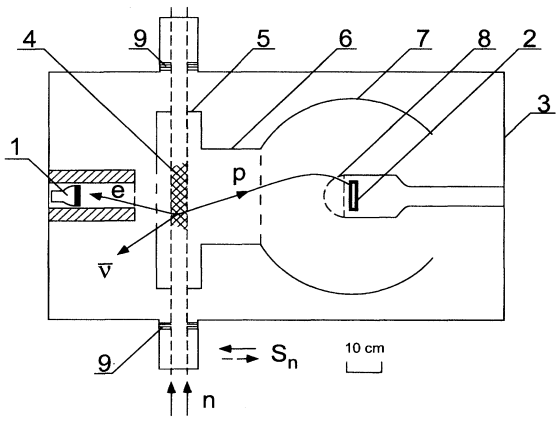

FIG. 2. Experimental apparatus. (1) Electron detector, (2) proton detector, (3) vacuum chamber, (4) decay region, (5) cylindrical electrode, (6) TOF electrode, (7) spherical electrode, (8) spherical grid, and (9) LiF diaphragm.

of acquisition time, a total of 393 057 decay events were registered. At the maximum of the time of flight spectrum, the signal to noise ratio was 15 to 1.

The electron energy detector is calibrated at the beginning and end of every run. This is done to correct for possible gain shifts of the photomultiplier. Calibrations are carried out with two calibrated electron sources ^{113}Sn (357 keV) and ^{137}Cs (617 keV).

Comparisons of experimental results and calculations for both time and energy spectra are shown in Fig. 3. The proton time of flight spectrum is integrated over energy and polarization states, while the energy spectrum is integrated over time and polarization states. There is good agreement between experimental and calculated time of flight spectra [$\chi^2/(N-1) = 1.15$]. The agreement between the energy spectra in the region of low energy is poor, possibly due to nonlinearities in the electronics in this region, but an analysis of this discrepancy shows that it does not influence the final result.

To extract PB from the data, the Monte Carlo and experimental time spectra are divided into a number of parts with each containing equal intensity. Each of these parts corresponds to a unique *energy independent* value of $\cos\Theta_{\sigma\bar{\nu}}$. Use of this method renders us insensitive to shifts or nonlinearities in the time scales. Finally, averaging corresponding parts over energy we obtain PB as a function of $\cos\Theta_{\sigma\nu}$ (see Fig. 4). Statistically combining these results, we obtain $PB = 0.6617 \pm 0.0044$ for $\chi^2/(N-1) = 0.78$.

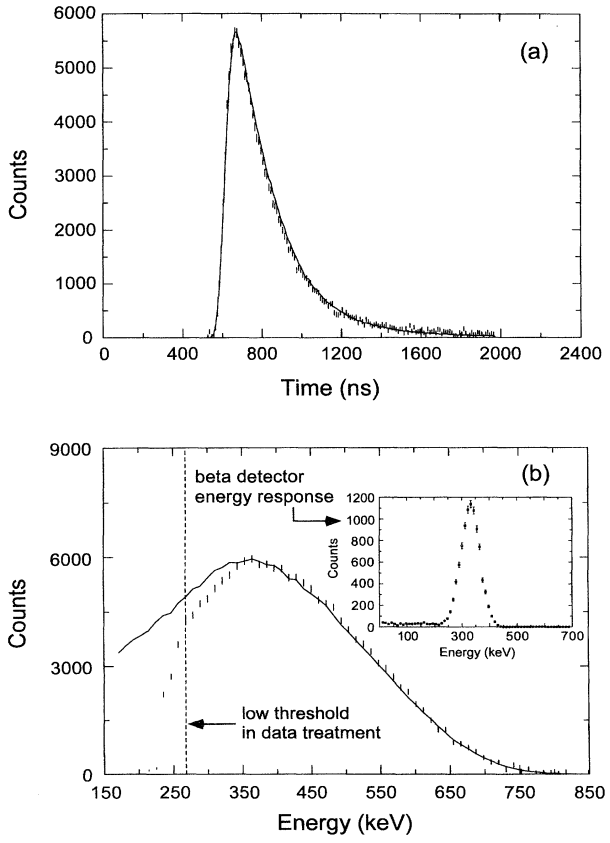

FIG. 3. Comparison of experimental and simulated spectra. (a) Time of flight spectra and (b) energy spectra including the measured beta detector energy response. Vertical lines are experimental points; the solid curve is a computer simulation.

Possible systematic errors in this experiment are analyzed by varying model parameters in the Monte Carlo by an amount equal to the experimental uncertainty on those parameters. Table I includes a list of errors. From the analysis we conclude that the total systematic error on our result is 0.0038. The largest source of uncertainty (± 0.0021) is due to the poor energy resolution of electron detector (25% for 115 keV).

The polarization of the neutron beam was measured using a new high precision technique [10]. In these measurements both the beam velocity spectrum and angular distribution are taken into account. The measured wavelength-dependent polarization is averaged with the time of flight spectrum through the apparatus. An additional correction is made to take into account the spectral dependence of the neutron spin flipper efficiency. The polarization measurements were carried out simultaneously with the measurement of B. From these measurements a value of the polarization was obtained:

$$P = 0.6688 \pm 0.0022. \quad (4)$$

Using the value of PB and P, we find

$$B = 0.9894 \pm 0.0083. \quad (5)$$

The accuracy of this result is 4.5 times better than the previous measurement [11]. The two results are consistent.

The antineutrino spin asymmetry B is not sensitive to influences from the strong interactions, to renormalization of the axial vector constant, or to influences of radiative corrections. B varies from 0.988 by less than 0.001

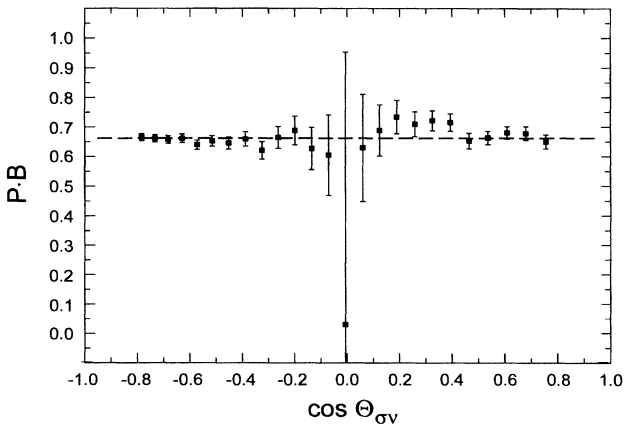

FIG. 4. Dependence of B on $\cos\Theta_{\sigma\nu}$. The average value $PB = 0.6617 \pm 0.0044$ and $\chi^2/(N-1) = 0.78$.

TABLE I. Final 1σ absolute uncertainties on B. The total systematic error is the quadrature sum of the individual errors. The total absolute error is the quadrature sum of the systematic, polarization, and statistical errors.

Source of uncertainty	Nominal value	Uncertainty	Uncertainty on B
^{113}Sn position (channels)	18.25	0.3	0.0026
Energy resolution of electron detector (keV)	34.5	1.7	0.0020
Size of energy channel (keV)	10.75	0.13	0.0007
Electron backscattering fraction	0.06	0.02	0.0012
Radius of proton detector diaphragm (mm)	130.0	0.25	0.0004
Radius of electron detector (mm)	37.5	0.25	0.0001
Radius of electron detector diaphragm (mm)	45.0	0.25	0.0006
Electron neutrino asymmetry (a)	0.1017	0.0051	0.0010
Electron spin polarization asymmetry (A)	−0.1126	0.0011	0.0005
Total systematic error			0.0038
Polarization error			0.0033
Statistical error			0.0066
Total absolute error			0.0083

when it is evaluated according to V-A theory using the discrepant values of $\lambda = g_a/g_v$ from different experiments. As a consequence of this, it is possible to place a restriction on the mass of W_R using B alone. In the left-right symmetric model with zero mixing angle one has $B = (1 - 2\delta^2)B_{V\text{-}A}$ where δ is the squared ratio of left- to right-handed boson masses. For this deviation, our measured value with its accuracy of 0.84% constrains M_{W_R} to be greater than or equal to 281 GeV/c^2 (90% C.L.). General restrictions in the squared mass ratio (δ) mixing angle (ζ) plane arising from this experimental result are shown in Fig. 5. The figure includes experimental results for the neutron lifetime, neutron electron spin asymmetry, lifetime for $0^+ \rightarrow 0^+$ transitions, and lifetime and asymmetry in ^{19}Ne, which together suggest a mass of about 230 GeV/c^2 for W_R. The results of this direct neutron beta decay experiment fail to confirm the existence of a finite δ at zero mixing angle.

With more statistics, improved energy resolution, and better beam polarization, we hope to improve this mass limit to 400 GeV/c^2.

This work was supported by ISF Grant No. 59000 and Grant No. 93-02-14382 of the Russian Fund of Fundamental Research.

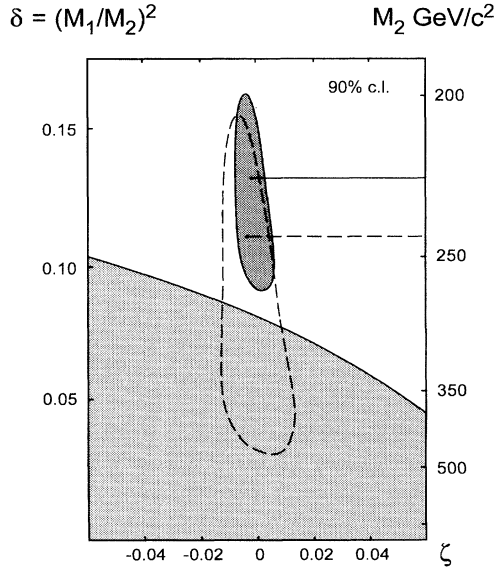

FIG. 5. Restrictions on the left-right symmetric model from different experimental data. (1) The darker shaded region comes from measurements of λ_τ and λ_A in the neutron and ^{19}Ne systems; (2) the region surrounded by a dotted line is the same except that data from Ref. [9] are not used; (3) the lighter shaded region comes from the present measurement.

[1] D. Dubbers, W. Mampe, and J. Döhner, Europhys. Lett. **11**, 195 (1990).
[2] A. S. Carnoy, J. Deutsch, T. A. Girard, and R. Prieels, Phys. Rev. Lett. **65**, 3249 (1990).
[3] A. P. Serebrov and N. V. Romanenko, JETP Lett. **55**, 503 (1992).
[4] A. Jodidio *et al.*, Phys. Rev. D **34**, 1967 (1986).
[5] UA2 Collaboration, J. Alitti *et al.*, Nucl. Phys. **B400**, 3 (1993).
[6] B. G. Erozolimsky, Y. A. Mostovoi, and A. I. Frank, I. V. Kurchatov Institute of Atomic Energy, Moscow Report No. IAE-3180, 1979.
[7] J. D. Jackson, S. B. Treiman, and H. W. Wyld, Phys. Rev. **106**, 517 (1957).
[8] C. Stratowa, R. Dobrozemsky, and P. Weinzierl, Phys. Rev. D **18**, 3970 (1978).
[9] B. G. Erozolimskii, I. A. Kuznetsov, I. A. Kuida, Y. A. Mostovoi, and I. V. Stepanenko, Sov. J. Nucl. Phys. **52**, 999 (1990).
[10] A. P. Serebrov, A. V. Aldushchenkov, M. S. Lasakov, I. A. Kuznetsov, and I. V. Stepanenko, "New Method for Precise Determination of Neutron Beam Polarization," Nucl. Instrum. Methods Phys. Res., Sect. A (to be published).
[11] B. G. Erozolimskii *et al.*, Yad. Fiz. **12**, 323 (1970).